Production of four-quark states with double heavy quarks at LHC

Yu-Qi Chen and Su-Zhi Wu*

Key Laboratory of Frontiers in Theoretical Physics,

Institute of Theoretical Physics, Chinese Academy of Sciences

Beijing 100190, P.R. China

Abstract

We study the hadronic production of four-quark states with double heavy quarks and double light antiquarks at LHC. The production mechanism is that a color anti-triplet diquark cluster consisting of double heavy quarks is formed first from the produced double heavy quark-antiquark pairs via gg fusion hard process, followed by the fragmentation of the diquark cluster into a four-quark (tetraquark) state. Predictions for the production cross sections and their differential distributions are presented. Our results show that it is quite promising to discover these tetraquark states in LHC experiments both for large number events and for their unique signatures in detectors.

keyword: tetraquark, diquark, heavy quark, fragmentation, production

1 Introduction

LHC experiments provide the unique opportunity to explore some exotic states of heavy quarks. Among them, particularly interesting states are those four-quark states consisting of double heavy quarks and double light antiquarks (or their charge

*zzswu@itp.ac.cn

conjugator). The existence of such states can be inferred from the heavy quark symmetry. The double heavy quarks in the color anti-triplet state may form a diquark cluster by the attractive strong interactions. In the heavy quark limit, the double heavy quarks move slowly in a small relative velocity v in the rest frame within a smaller distance $(1/mv)$, comparing to the size of light degree of freedom $(1/\Lambda_{QCD})$. Thus in the tetraquark states the double heavy quarks form a color anti-triplet diquark cluster. It contributes the color interactions to double light antiquarks as a color source of a heavy antiquark. The other two light antiquarks move around it with attractive interactions between them. The dynamics of the light degrees of freedom of these tetraquark states are similar with those of the heavy baryons. The picture is supported by scrutinizing the typical sizes of real hadrons. The size of the heavy quarkonium is around $0.2 - 0.3$ fm while that of the light hadrons is around 1 fm. The masses of such states can be roughly estimated as the sum of two heavy quarks' masses and Λ_{QCD}. For the tetraquark states containing the cc, cb, and bb quarks, their masses are around 3.4 GeV, 6.8 GeV, and 10.2 GeV, respectively. The flavor features of this sort of hadrons are very different from the conventional hadrons. Once they are discovered in experiments, it will be an undoubted evidence for the existence of the tetraquark states. Some theoretical studies on these states were presented in literatures[1, 2, 3, 4, 5, 6].

The spin of a tetraquark state is a composition of the spins of the four quarks and the relative orbital angular momenta between them. For $S-$waves, all orbital angular momenta vanish. Then the spin of the tetraquark state is just the composition of the spin of each quark or antiquark. The composition of the spins of double heavy quarks may be 0 or 1. However, when two heavy quarks are identical, only spin 1 state is allowed due to the antisymmetry by exchanging identical fermions. It is also the same case for the light antiquarks sector. In this paper, we are interested in only the tetraquark states with all orbital angular momenta vanishing. We denote states by $T^i_{Q_1Q_2}$ (i=0, 1) , where Q_1 and Q_2 represent their heavy flavor indexes and i is the spin of the double heavy quarks subsystem.

As bound states with quite large masses they are difficult to be produced at usual high energy machines. Nevertheless, at LHC, they can be produced efficiently via a direct production process which involves effects happened at several distinct distance

scales. Firstly, two heavy quark-antiquark pairs are produced via gluon-gluon fusion hard subprocess at distance scale $1/m$ or shorter. Secondly, for those produced two heavy quarks with small relative velocity v there are certain probabilities to form a color anti-triplet diquark cluster at distance scale $1/mv$. Finally the diquark cluster evolves into the tetraquark state via the fragmentation process by picking up two light antiquarks from the vacuum at the distance scale $1/\Lambda_{QCD}$.

In this paper, we calculate the hadronic production cross sections of T^1_{cc}, T^i_{bc} (i=0, 1), and T^1_{bb} via gluon-gluon fusion process at LHC. Our results show that a number of these particles can be produced. We also point out the signatures to detect those particles.

The rest of the paper are organized as follows. In Sec. 2, we present the calculation of the subprocess $gg \to T^i_{Q_1Q_2}\bar{Q}_1\bar{Q}_2 + X$. Sec. 3 devotes to the numerical results of the cross sections of the tetraquark states at LHC and at Tevatron. In Sec. 4, we give some discussions about the results and the signals in the detectors.

2 Cross section of $gg \to T^i_{Q_1Q_2}\bar{Q}_1\bar{Q}_2 + X$

As mentioned above, in the production process of the tetraquark states $T^i_{Q_1Q_2}$, there are three hierarchy distance scales, i.e., $1/m \ll 1/mv \ll 1/\Lambda_{QCD}$. Accordingly, the cross sections of the subprocesses for the production of the $S-$wave tetraquark states, $T^i_{Q_1Q_2}$, can be factored into three different parts accounting for physical effects happening at those distinct distance scales:

$$\widehat{\sigma}(gg \to T^i_{Q_1Q_2}) = \frac{1}{2\hat{s}}\frac{1}{64d}\int d\Pi_3\, C_{\bar{3}}(\alpha_s, Q_1Q_2)\,|\Psi_{\bar{3}}(0)|^2 \int_0^1 dx D_{\bar{3}\to T^i_{Q_1Q_2}}(x), \qquad (1)$$

where $d = 1$ for T^0_{bc} and T^1_{bc}, and $d = 2$ for T^1_{bb} and T^1_{cc}; $\hat{s}$ is the squared invariant mass of the double gluons; $d\Pi_3$ is the Lorentz invariant three-body phase space integral element; $C_{\bar{3}}(\alpha_s, Q_1Q_2)$ is the short-distance coefficient describing the production rate of the color anti-triplet point-like Q_1Q_2 state at the energy scale m or higher; $\Psi_{\bar{3}}(0)$ is the wave function at the origin of the $S-$wave diquark state; $D_{\bar{3}\to T^i_{Q_1Q_2}}(x)$ is the fragmentation function of the diquark into the color-singlet tetraquark state $T^i_{Q_1Q_2}$.

The short-distance coefficient can be calculated by perturbative QCD and can be expanded in terms of α_s at the short-distance energy scale m or higher. The

rest parts are non-perturbative effects in nature. To estimate the production cross sections, one needs to determine their numerical values. The formation of the diquark cluster from the free double heavy quarks is described by the wave function at the origin. Their numerical values can be estimated by the potential model. The diquark cluster provides an anti-triplet color source as a heavy antiquark. Thus, in the heavy quark limit, its fragmentation probability for forming the tetraquark states can then be approximately described by that for forming the heavy baryons by a heavy quark.

In this paper, we calculate the cross sections of hadronic production of the $S-$wave states, T^1_{cc}, T^1_{bc}, T^0_{bc}, and T^1_{bb}, at LHC. We compute the tree level short-distance coefficients $C_{\bar{3}}(\alpha_s, Q_1Q_2)$ in the leading order α_s^4 using perturbation QCD. By estimating the nonperturbative matrix elements, we carry out the numerical calculations of the total cross sections. Our results show that a number of these particles can be produced.

We first calculate the short-distance coefficients $C_{\bar{3}}(\alpha_s, Q_1Q_2)$ at the tree level. They are proportional to the squared matrix elements $M(gg \to (Q_1Q_2)_{\bar{3}})$. To calculate the matrix elements, one needs to calculate the subprocess of $gg \to Q_1Q_2\bar{Q}_1\bar{Q}_2$, with Q_1 and Q_2 moving in the same $3-$velocity and in the color anti-triplet state. At the tree level, the production processes involve 36 Feynman diagrams for $gg \to bc\bar{b}\bar{c}$, and 72 ones for $gg \to bb\bar{b}\bar{b}$ and $gg \to cc\bar{c}\bar{c}$. The amplitudes can be classified as six gauge-invariant subsets in terms of six independent color bases. Given this, the calculations of the amplitudes as well as their squares are straightforward.

$\Psi_{\bar{3}}(0)$'s are the wave functions at the origin of the S-wave diquark clusters. Their precise values are difficult to be gained since the large range interaction potential between the double heavy quarks in the color anti-triplet state is not very clear while the short range one is dominated be Coulomb potential. Reasonably, we take values predicted by solving Schödinger equation with Coulomb potential, $v(r) = -2\alpha_s/(3r)$. Then the predicted $\Psi_{\bar{3}}(0)^2$'s are 0.143, 0.0382, and 0.0198 GeV^3 for bb, bc, and cc diquark systems, respectively. Including the confinement part, the wave function is squeezed to the central region and hence the wave function at the origin will be enhanced. Actually, we have done numerical calculations for the diquark state by solving the Schrödinger equation using Coulomb potential plus the linear potential fixed in the color-singlet case, the numerical value of wave function at the origin is

enhanced by 10% - 30%. More reliable prediction for this nonperturbative number can be obtained by some nonperturbative method like lattice QCD.

We now turn to the fragmentation function of $(Q_1Q_2)_{\bar{3}}$-cluster to a tetraquark state. As discussed above, the produced heavy diquark cluster in the color anti-triplet state provides the same color source as the heavy antiquark to the light antiquarks in the limit of the ratio of size of the diquark over that of the light antiquarks in the tetraquark state. Thus the fragmentation probabilities to produce the tetraquark states $T^i_{Q_1Q_2}$ from the heavy diquarks are the same with that to produce the heavy baryons from the heavy quarks. Let's take a QED example to illustrate it. Imagine the hydrogen ion or deuterium ion passing material. The probabilities forming the hydrogen atom or the deuterium one are the same if the velocities of both ions are the same since they possess the same electric charge. The fragmentation function is defined in the framework of the infinity momentum where the parton moves in the speed of light.

The fragmentation functions to produce the tetraquark states are nonperturbative in nature. Thus the shapes of them can only be described by certain phenomenological models [7, 8]. One of the most commonly used models is the Peterson model[7], in which the fragmentation function takes the following form:

$$D_{\bar{3}} \to T^i_{Q_1Q_2}(x) = \frac{N}{x[1-(1/x)-\epsilon_{Q_1Q_2}/(1-x)]^2} \tag{2}$$

where $\epsilon_{Q_1Q_2}$ is the only parameter determining the shape of the fragmentation function; N is the normalization constant. Once the fragmentation probability to produce the tetraquark state R is given, N is fixed by the following condition:

$$\int dx\, D_{\bar{3}} \to T^i_{Q_1Q_2}(x) = R, \tag{3}$$

The fragmentation probabilities of $c \to \Lambda_c$ and $b \to \Lambda_b$ have been measured in e^+e^- collisions [9, 10, 11]. According to PDG 2006 [9], $R(c \to \Lambda_c) = 0.094 \pm 0.035$, and $R(b \to \Lambda_b) = 0.099 \pm 0.017$. These results are about 0.1. Therefore as a good approximation we may take the fragmentation probability of $(Q_1Q_2)_{\bar{3}} \to T^i_{Q_1Q_2}$, the value of R in Eq.(3), be 0.1.

From Eqs.(2) and (3) we know the normalization constant N in the Peterson model is dependent on the parameter ϵ_Q. The model suggested a scaling behavior for

the parameter ϵ_Q that is proportional to $1/m_Q^2$. The ϵ_b determined by experiments is about $0.003 \sim 0.006$ [10, 12]. Using the scaling behavior and taking ϵ_b to be 0.004, we predict that $\epsilon_{bc} = (\frac{m_b}{m_{bc}})^2\epsilon_b \simeq 0.0023$, $\epsilon_{cc} = (\frac{m_b}{m_{cc}})^2\epsilon_b \simeq 0.011$, $\epsilon_{bb} = (\frac{m_b}{m_{bb}})^2\epsilon_b = 0.001$ and the corresponding normalization constants are 0.0075, 0.0194, 0.0047. Here we take $m_b = 4.9$ GeV, $m_c = 1.5$ GeV and $m_{(Q_1Q_2)} = m_{Q_1} + m_{Q_2}$.

The fragmentation functions are energy scale dependent. Their convolution from one energy scale to another satisfies DGLAP equation. However, for the hadronic production of the tetraquark states at LHC, the production is dominated by the smaller P_T region of the produced particles, i.e., compatible with the tetraquark masses. For smaller P_T production of the tetraquark state, there are no distinguishable energy scale differences. Thus the evolution of the fragmentation function used here is not significant. Therefore, in the numerical calculations we can take the fragmentation functions with the initial energy scale to be the tetraquark mass without evolution.

3 Numerical results of the cross sections of the tetraquark states at LHC

We now turn to the calculation of the total cross sections with $\hat{\sigma}$ of the subprocess given in Eq. (1). According to the parton model, the cross sections of the processes $pp \to T^i_{Q_1Q_2} + \bar{Q}_1 + \bar{Q}_2 + X$, can be expressed as:

$$\frac{d\sigma}{dP_T} = \int dx_1 dx_2 f_{g_1}(x_1, \mu_F) f_{g_2}(x_2, \mu_F) \frac{d\widehat{\sigma}}{dP_T}(gg \to T^i_{Q_1Q_2}, \mu_F)\,, \tag{4}$$

where μ_F is the factorization energy scale, P_T is the transverse momentum of the $T^i_{Q_1Q_2}$, and $f_g(x, \mu_F)$ is the distribution function of the gluon in the proton. Here we use the cteq6l [13] parton distribution function. There is an uncertainty in the calculations arising from the choice of the factorization energy scale μ_F. Here for comparison, we take two different values of μ_F, i.e., $\mu_F = \mu_R$ and $\mu_R/2$, where $\mu_R^2 = p_{TQ_1Q_2}^2 + m_{Q_1Q_2}^2$ with $p_{TQ_1Q_2}$ being the transverse momentum of the diquark. With the choices of these factorization energy scales and α_s given in [14] for the cteq6l [13] parton distribution function, we calculate the total cross sections in CMS, ATLAS and LHCb with the invariant mass of the pp system, $\sqrt{s} = 7$ TeV and 14 TeV,

Table 1: The predicted hadronic production cross sections (in unit nb) of the tetraquark states with various P_T cuts at LHC with $\sqrt{s}$=14 TeV. The pseudo-rapidity cuts $|\eta| < 2.5$ for CMS and ATLAS, and $1.9 < \eta < 4.9$ for LHCb are taken.

-	-	LHC (CMS, ATLAS)		LHCb	
-	η-cut / P_T-cut	$\|\eta\| < 2.5$		$1.9 < \eta < 4.9$	
	μ_F=	μ_R	$\mu_R/2$	μ_R	$\mu_R/2$
T^0_{bc}	0 GeV	0.460	0.643	0.263	0.374
-	5 GeV	0.167	0.238	0.0590	0.0865
-	10 GeV	0.0286	0.0429	0.0077	0.0118
T^1_{bc}	0 GeV	1.73	2.42	1.02	1.45
-	5 GeV	0.567	0.822	0.205	0.302
-	10 GeV	0.087	0.131	0.0235	0.0356
T^1_{bb}	0 GeV	0.129	0.193	0.0697	0.105
-	5 GeV	0.0758	0.114	0.0279	0.0430
-	10 GeV	0.0220	0.0339	0.00598	0.0093
T^1_{cc}	0 GeV	35.6	37.8	24.6	25.7
-	5 GeV	1.29	1.84	0.414	0.629
-	10 GeV	0.072	0.113	0.0178	0.0274

respectively. The numerical results of the total production cross sections are listed in Tables 1 and 2. The P_T and the rapidity distributions are shown in Figs.1-6. From Tables 1 and 2, we see that the total cross section to produce T^1_{cc} without P_T-cut is much larger than the one with $P_T > 5.0$ GeV. This can be explained with two reasons, i.e., the small peak value in the P_T distribution of the subprocess $gg \to T^1_{cc}$ and the shape of fragmentation function of $cc-$cluster. They also result in the lines of the P_T-distributions across in Figs.(1), (2), (4), and (5) .

From Table 1, we see that for LHC with 300 fb^{-1} integrated luminosity running at 14 TeV, for the production of T^1_{cc}, around $(3.9 - 5.5) \times 10^8$ events in CMS and ATLAS can be accumulated with kinematic cuts $P_T > 5$ GeV and $|\eta| < 2.5$, while this number is around $(1.2-1.9)\times 10^8$ with kinematic cuts $P_T > 5$ GeV and $1.9 < \eta < 4.9$

Table 2: The predicted hadronic production cross sections (in unit nb) of the tetraquark states with various P_T cuts at LHC with $\sqrt{s}$=7 TeV . The pseudo-rapidity cuts $|\eta| < 2.5$ for CMS and ATLAS, and $1.9 < \eta < 4.9$ for LHCb are taken.

-	-	LHC (CMS, ATLAS)		LHCb	
-	η-cut / P_T-cut	$\|\eta\| < 2.5$		$1.9 < \eta < 4.9$	
	μ_F=	μ_R	$\mu_R/2$	μ_R	$\mu_R/2$
T^0_{bc}	0 GeV	0.228	0.352	0.117	0.184
-	5 GeV	0.0766	0.121	0.0221	0.0358
-	10 GeV	0.0119	0.0195	0.00243	0.00407
T^1_{bc}	0 GeV	0.860	1.33	0.456	0.717
-	5 GeV	0.265	0.416	0.0776	0.125
-	10 GeV	0.0364	0.0599	0.0075	0.0126
T^1_{bb}	0 GeV	0.0578	0.0936	0.0273	0.0448
-	5 GeV	0.0328	0.0535	0.0098	0.0164
-	10 GeV	0.0088	0.0145	0.00180	0.00304
T^1_{cc}	0 GeV	20.8	25.9	13.3	16.3
-	5 GeV	0.630	1.01	0.166	0.272
-	10 GeV	0.030	0.051	0.00580	0.0099

in LHCb. For the production of T_{bc}, both T_{bc}^0 and T_{bc}^1 need to add together since the higher mass state will decay into the lower mass state by emitting a photon. After doing this, we see that for 300 fb^{-1} integrated luminosity running at 14 TeV, for the production of T_{bc}, around $(2.2-3.2)\times 10^8$ events in CMS and ATLAS can be accumulated with kinematic cuts $P_T > 5$ GeV and $|\eta| < 2.5$, while this number is around $(0.8-1.2)\times 10^8$ with kinematic cuts $P_T > 5$ GeV and $1.9 < \eta < 4.9$ in LHCb. For the production of T_{bb}^1, around $(2.2-3.4)\times 10^7$ events in CMS and ATLAS can be accumulated with kinematic cuts $P_T > 5$ GeV and $|\eta| < 2.5$, while this number is around $(0.8-1.3)\times 10^7$ with kinematic cuts $P_T > 5$ GeV and $1.9 < \eta < 4.9$ in LHCb.

From Table 2, we see that for 10 fb^{-1} integrated luminosity running at 7 TeV, for the production of T_{cc}^1, around $(0.6-1.0)\times 10^7$ events in CMS and ATLAS can be accumulated with kinematic cuts $P_T > 5$ GeV and $|\eta| < 2.5$, while this number is around $(1.6-2.7)\times 10^6$ with kinematic cuts $P_T > 5$ GeV and $1.9 < \eta < 4.9$ in LHCb. For the production of T_{bc}, both T_{bc}^0 and T_{bc}^1 need to add together also. After doing this, we see that for 10 fb^{-1} integrated luminosity running at 7 TeV, for the production of T_{bc}, around $(3.4-5.4)\times 10^6$ events in CMS and ATLAS can be accumulated with kinematic cuts $P_T > 5$ GeV and $|\eta| < 2.5$, while this number is around $(1.0-1.6)\times 10^6$ with kinematic cuts $P_T > 5$ GeV and $1.9 < \eta < 4.9$ in LHCb. For the production of T_{bb}^1, around $(3.3-5.4)\times 10^5$ events in CMS and ATLAS can be accumulated with kinematic cuts $P_T > 5$ GeV and $|\eta| < 2.5$, while this number is around $(1.0-1.6)\times 10^5$ with kinematic cuts $P_T > 5$ GeV and $1.9 < \eta < 4.9$ in LHCb.

We also calculate the total cross sections at Tevatron with $\sqrt{s} = 1.96$ TeV . The numerical results of the total production cross sections are listed in Table 3. The P_T-distributions and the rapidity distributions are shown in Figs.7 and 8.

From Table 3, we see that for 2 fb^{-1} integrated luminosity running at 1.96 TeV, for the production of T_{cc}^1, around $(0.8-1.6)\times 10^5$ events at Tevatron can be accumulated with kinematic cuts $P_T > 5$ GeV and $|y| < 0.6$. For the production of T_{bc}, again by adding both T_{bc}^0 and T_{bc}^1 events together, we see that for 2 fb^{-1} integrated luminosity, for the production of T_{bc}, around $(0.4-0.8)\times 10^5$ events at Tevatron can be accumulated with kinematic cuts $P_T > 5$ GeV and $|y| < 0.6$. For the production of T_{bb}^1, around $0.4-0.7\times 10^4$ events at Tevatron can be accumulated with kinematic cuts $P_T > 5$ GeV and $|y| < 0.6$.

Table 3: The predicted hadronic production cross sections (in unit nb) of the tetraquark states with various P_T cuts at Tevatron with $\sqrt{s}$=1.96 TeV .The rapidity cut $|y| < 0.6$.

μ_F	P_T cut	T^1_{cc}	T^1_{bc}	T^0_{bc}	T^1_{bb}
μ_R	0 GeV	3.01	0.0832	0.0219	0.00436
-	5 GeV	0.041	0.0168	0.00487	0.00182
-	10 GeV	0.00149	0.00178	0.00058	0.00039
$\mu_R/2$	0 GeV	5.01	0.157	0.0410	0.00837
-	5 GeV	0.081	0.0312	0.0090	0.00352
-	10 GeV	0.0029	0.00339	0.0011	0.00075

There are some uncertainties in the predicted numerical results. One arises from the ambiguity in choosing the factorization energy scale μ_F. From the Tables, we see that two different values of μ_F lead to around and less than factor 2 difference in the cross section. The next leading order result will reduce this uncertainty. However, it will be very hard calculation. Another one arises from the wave function at the origin, as discussed in Sec. 2, it will increase the cross sections by 20-70 % including the linear confinement potential between the heavy quark. Moreover, all excited heavy diquark states will decay into the ground diquark states by emitting photons or π's. Including those contributions, the production cross sections may be enhanced by 2-3 times.

Comparing the P_T distributions at LHC and Tevatron, we see that the differential cross sections decrease faster at Tevatron than at LHC with the P_T increase.

In calculating the accumulated events number, we take the integrated luminosity as the corresponding collider running at present or planning luminosity for about one year. From the above discussions, we see that the predicted event number of the tetraquark at the Tevatron is about 3-4 orders of magnitude lower than that at LHC with $\sqrt{s} = 14$ TeV for one year.

The events can be discovered at Tevatron is much smaller than the ones can be discovered at LHC, especially when the energy and luminosity of LHC reach the maximum.

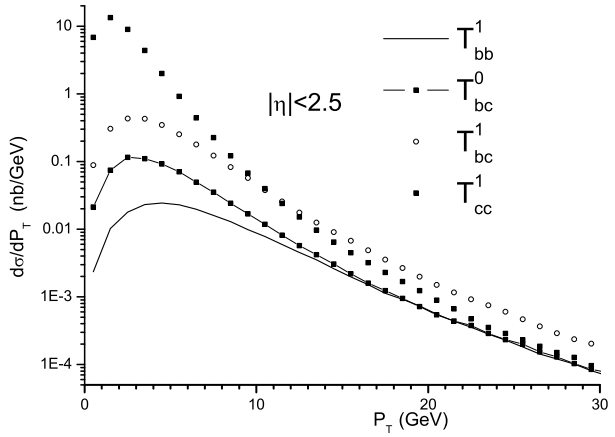

Figure 1: The predicted P_T-distributions of the tetraquark states, T^1_{bb}, T^1_{cc}, T^0_{bc} and T^1_{bc}, in CMS and ATLAS with $\sqrt{s}$=14 TeV, with the pseudo-rapidity cut $|\eta| < 2.5$ and μ_F=$\mu_R/2$.

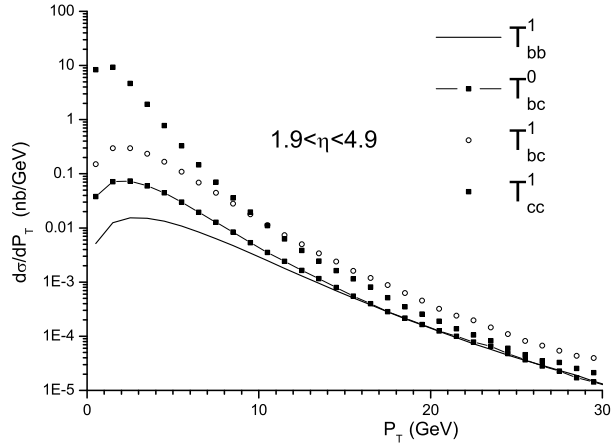

Figure 2: The predicted P_T-distributions of the tetraquark states, T^1_{bb}, T^1_{cc}, T^0_{bc} and T^1_{bc}, in LHCb at $\sqrt{s}$=14 TeV, with the pseudo-rapidity cut $1.9 < \eta < 4.9$ and μ_F=$\mu_R/2$.

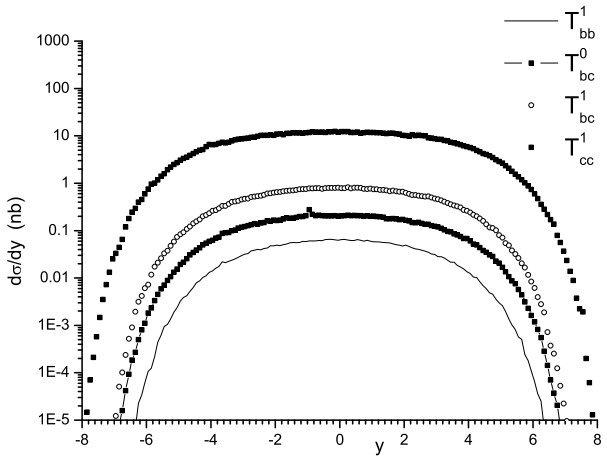

Figure 3: The predicted rapidity distributions of the tetraquark states, T^1_{bb}, T^1_{cc}, T^0_{bc} and T^1_{bc}, with μ_F=$\mu_R/2$, at LHC with $\sqrt{s}$=14 TeV.

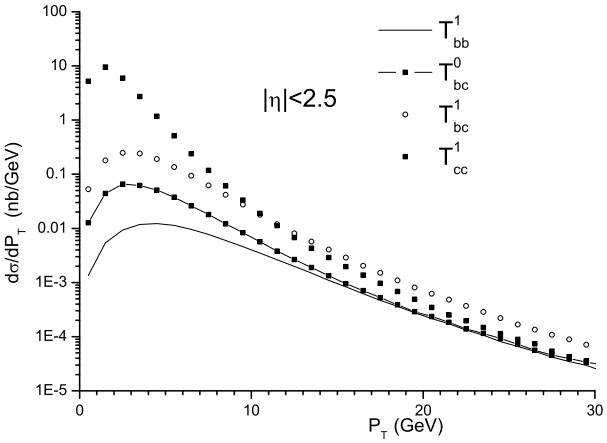

Figure 4: The predicted P_T-distributions of the tetraquark states, T^1_{bb}, T^1_{cc}, T^0_{bc} and T^1_{bc}, in CMS and ATLAS at $\sqrt{s}$=7 TeV, with the pseudo-rapidity cut $|\eta| < 2.5$ and μ_F=$\mu_R/2$.

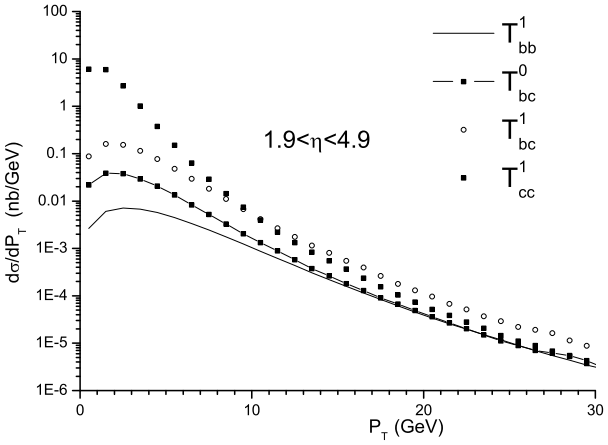

Figure 5: The predicted P_T-distributions of the tetraquark states, T^1_{bb}, T^1_{cc}, T^0_{bc} and T^1_{bc}, in LHCb at $\sqrt{s}$=7 TeV, with the pseudo-rapidity cut $1.9 < \eta < 4.9$ and μ_F=$\mu_R/2$.

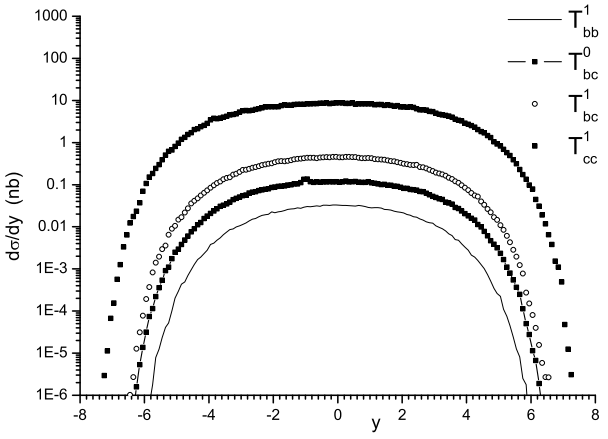

Figure 6: The predicted rapidity distributions of the tetraquark states, T^1_{bb}, T^1_{cc}, T^0_{bc} and T^1_{bc} with μ_F=$\mu_R/2$, at LHC with $\sqrt{s}$=7 TeV.

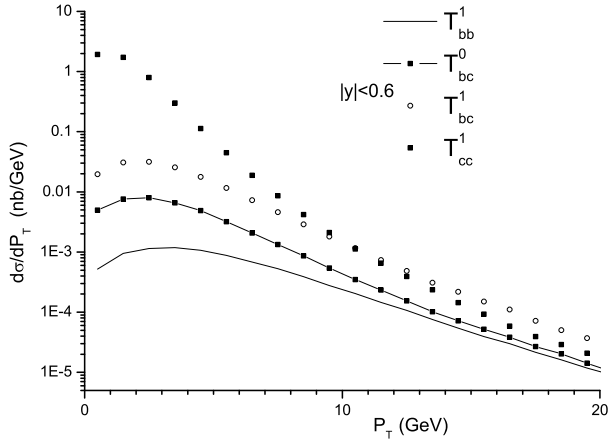

Figure 7: The predicted P_T-distributions of the tetraquark states, T^1_{bb}, T^1_{cc}, T^0_{bc} and T^1_{bc}, at Tevatron with $\sqrt{s}$=1.96 TeV, with the rapidity cut $|y| < 0.6$ and μ_F=$\mu_R/2$.

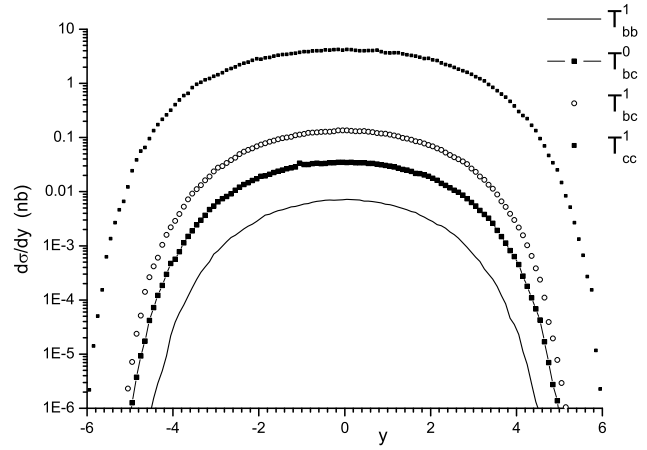

Figure 8: The predicted rapidity distributions of the tetraquark states, T^1_{bb}, T^1_{cc}, T^0_{bc} and T^1_{bc} with μ_F=$\mu_R/2$, at Tevatron with $\sqrt{s}$=1.96 TeV.

4 Signature and summary

The decays of the tetraquark states with double heavy quarks possess unique signatures in the detectors. To analyze them in detail is very useful for probing them in experiments. For the ground tetraquark states, they can not decay by the strong and the electro-magnetic interactions. However, they can decay through the weak interaction. The inclusive decay can be regards as the cascade weak decays of the heavy quarks while the light antiquarks are spectators. When the leptons can easily be identified in detectors, we focus on those semileptonic decays of the heavy quarks in the tetraquark states.

Now we analyze the semileptonic decays of the $T^i_{Q_1Q_2}$ states one by one. By weak interaction, the c quark can decay to s quark by emitting the e^+ or μ^+, and an invisible neutrino. In the T^1_{cc}, double c quarks decay in this way independently, with the two antiquarks as spectators. The emitted same plus sign double leptons and the P_T-distributions can be used to deduce the background.

In the T^i_{bc}, there are two heavy quarks with different flavors. Both the c and the b quarks have the semi-leptonic decay modes. As discussed in the last paragraph, the c quark can decay to s quark by emitting, e^+ or μ^+, and an invisible neutrino. The b quark can decay to the c quark by emitting the e^-, μ^-, or τ^- lepton and the corresponding invisible anti-neutrino, followed by the c quark decays as above. As a result, the two plus sign leptons and one lepton can be detected from those cascade decays, giving the special signature for identifying the T^i_{bc}.

The inclusive semi-leptonic decay of T^1_{bb} is somewhat more complicated. Each b quark can decay to the c quark with a lepton, e^-, μ^-, or τ^- and the corresponding invisible anti-neutrino, followed by the c quark decays as above. These leptons, two leptons and two plus sign leptons, provide the unique signature for identifying the T^1_{bb} state.

The decay vertexes and the $b-$tagging method will be very useful for identity those tetraquark states. Some other useful decays for identifying those tetraquark states are those 3-body or 4-body nonleptonic decays.

Considering the signatures and the efficiencies of the the detectors, we see that LHC with high luminosity running at 14 TeV provides best opportunity to discover

doubly heavy tetraquark states. In conclusion, our results show that it is quite promising to discover these tetraquark states in LHC experiments both for large number events and for their unique signatures in detectors. Once they are discovered in experiments, it will be an undoubted evidence for the existence of the tetraquark states. This will start a new stage in hadron physics.

Acknowledgments: This work is partly supported by the NSFC with the contract 10875156.

References

[1] S. Zouzou, B. Silvestre-Brac, C. Gignoux and J. M. Richard, Z. Phys. C **30**, 457 (1986).

[2] J. Vijande, A. Valcarce, and J.-M. Richard, Phys. Rev. D **76**, 114013 (2007).

[3] L. Heller and J. A. Tjon, Phys. Rev. D **35**, 969 (1987); J. Carlson, L. Heller and J. A. Tjon, Phys. Rev. D **37**, 744 (1988); A. V. Manohar and M. B. Wise, Nucl. Phys. B **399**, 17 (1993); S. Pepin, Fl. Stancu, M. Genovese and J. M. Richard, Phys. Lett. B **393**, 119 (1997).

[4] J.-P. Ader, J.-M. Richard and P. Taxil, Phys. Rev. D **25**, 2370 (1982); J. Vijande, A. Valcarce, J.-M. Richard and N. Barnea, hep-ph/0902.1657 (2009); J. Vijande, E. Weissman, A. Valcarce and N. Barnea, Phys. Rev. D **76**, 094027 (2007); M. Zhang, H. X. Zhang and Z. Y. Zhang, Commun. Theor. Phys. **50**, 437 (2008).

[5] Ernest Ma, James Pantaleone and S. Uma Sankar, Phys. Rev. D **46**, 463 (1992).

[6] J. Vijande, A. Valcarce, and N. Barnea, Phys. Rev. D **79**, 074010 (2009).

[7] C. Peterson, D. Schlatter, I. Schmitt, and P. M. Zerwas, Phys. Rev. D **27**, 105 (1983).

[8] V. G. Kartvelishvili, A. K. Likhoded and V. A. Petrov, Phys. Lett. B **78**, 615 (1978); M. G. Bowler, Z. Phys. C **11**, 169 (1981); P. Collins and T. Spiller, J. Phys. G **11**, 1289 (1985); G. Colangelo and P. Nason, Phys. Lett. B **285**, 167

(1992); E. Braaten, Kingman Cheung, Sean Fleming and Tzu Chiang Yuan, Phys. Rev. D **51**, 4819 (1995).

[9] Particle Data Group, J. of Phys. G 33 (2006), Review of Particle Physics. p200, p770.

[10] SLD Collaboration, K. Abe *et al.*, Phys. Rev. D **65**, 092006 (2002); DELPHI Collaboration, J. Abdallah *et al.*, hep-ex/0311005v1 (2003).

[11] CDF Collaboration, T. Affolder *et al.*, Phys. Rev. Lett. **84**, 1663 (2000); Anatoly Adamov and Gary R. Goldstein, Phys. Rev. D **56**, 7381 (1997).

[12] SLD Collaboration, K. Abe *et al.*, Phys. Rev. D **53**, 1023 (1996); ALEPH Collaboration, A. Heister *et al.*, Phys. Lett. B **512**, 30 (2001); The OPAL Collaboration, G. Abbiendi *et al.*, hep-ex/0210031v2.

[13] J. Pumplin, D. R. Stump, J. huston, H. L. Lai, P. Nadolsky, and W. K. Tung, hep-ph/0201195.

[14] $\alpha_s(Q) = \frac{b_0}{rat} \cdot (1 - b_1 \log(rat)/rat)$,
$\alpha_s(m_Z) = 0.118$, $\lambda_4 = 0.32$, $\lambda_5 = 0.223$,
$rat = \log(\frac{Q^2}{\lambda^2})$, $b_0 = \frac{12\pi}{33-2n_f}$, $b_1 = \frac{6\cdot(153-19n_f)}{(33-2n_f)^2}$,
$\lambda = \lambda_4$ and $n_f = 4$, When $Q < m_b$,
$\lambda = \lambda_5$ and $n_f = 5$, When $Q > m_b$.